

Tides of Global Ice-Covered Oceans

Preliminary Incomplete Draft

Carl Wunsch

Department of Earth and Planetary Sciences

Harvard University

Cambridge MA 02138

email: cwunsch@fas.harvard.edu

November 5, 2014

Abstract

The tides of an ice-covered ocean are examined using a Cartesian representation of the elastic and fluid equations. Although unconstrained by any observations, the ocean tides of a Neoproterozoic “snowball” Earth could be significantly larger than they are today. With the remaining ocean being substantially shallower than today, time-mean tidal-residual circulations could have been set up that are competitive with the circulation driven by geothermal heating. In any realistic configuration, the snowball Earth would have an ice cover that is in the thin shell limit, but by permitting the ice thickness to become large, more interesting ice tidal response can be found, ones conceivably of application to bodies in the outer solar system or hypothetical exoplanets.

1 Introduction

Several reasons exist for an exploration of the tides occurring in ice sheets, whether floating or land-confined. One reason is suggested by evidence that approximately 600 million years ago, during the Neoproterozoic, the entire Earth may have frozen, being everywhere covered with ice. Over the ocean a floating ice sheet may have existed with an estimated of several kilometers (the hard “snowball Earth”). Discussions of the evidence, primarily geological in nature, can be found in Hoffman and Schrag (2002). Ashkenazy et al. (2014; hereafter, A2014), describe a theoretical/modelling study of the oceanic circulation that might exist under an oceanic ice cover of order of several kilometers. The forcing they assume is purely geothermal, at the modern rate

24 of roughly $0.1\text{W}/\text{m}^2$ (Pollack et al., 1993; Davies, 2013), with some localized maxima over ridge-
 25 crests. They find an equatorially enhanced meridional overturning circulation, with transports
 26 up to 30Sv with a nearly homogeneous ocean, both in temperature and salinity. Some account
 27 is taken of the oceanic interaction with the overlying ice sheet.

28 Whether or not a snowball Earth actually existed, the question of what the ocean might be
 29 like under such circumstances is an interesting theoretical problem. A modern analogue is in the
 30 outer solar system satellites Enceladus and Europa which, also hypothetically, have fluid oceans
 31 covered by multi-kilometer thick ice sheets. In contrast to the A2014, solution, discussion of
 32 behavior of those oceans has centered on tidal forcing (Greenberg et al., 1998;...).

33 A comparatively large literature exists on tides induced in ice sheets by the oceanic tidal
 34 forcing at the outflow (e.g., Thomas, 2007; Arbic et al., 2008). In contrast, a tangential calcula-
 35 tion here is the body tide induced directly in very large ice sheets far from oceanic influence, and
 36 the tides induced in the ocean when overlain by an effectively infinitely thick ice cover. Some
 37 of the parameter ranges used here are far beyond anything reasonable for the Earth. Perhaps
 38 they have some relevance for another planet or satellite.

39 Dynamical discussion of continental scale ice sheets such as those in Antarctica and Green-
 40 land is difficult for a number of reasons, including the specification of the appropriate boundary
 41 conditions at the inaccessible bottom of the glacier. One can speculate that the tidal response
 42 observable at the glacier surface is sufficiently sensitive to the bottom boundary conditions that
 43 those conditions might be inferred.

44 2 A Cartesian Configuration

45 Because of all of the uncertainties of the physical setting of the Neoproterozoic Earth, the goal
 46 here is to understand the basic physics and to find orders of magnitude of the effects. Only a
 47 two-dimensional Cartesian system as in the Airy “canal theory” of water tides (Lamb, 1932), is
 48 used. Consider the situation in Fig. 1, in which an ice sheet of uniform thickness \bar{d} overlies an
 49 ocean of constant depth d . Below the ocean is an infinite elastic half-space. The fluid motion
 50 is computed with the half-space not moving, as if with the ocean tide being computed relative
 51 to the sea floor. Conceptually, as with ocean tides measured from tide gauges, tides within the
 52 elastic half-space will produce a modified tidal potential, $U = U_0(1 + k_L - h_L)$, where k_L, h_L
 53 are the conventional Love numbers (Munk and MacDonald, 1960; Lambeck, 1988). The net tide
 54 generating potential will be assumed to be,

$$U = gHe^{ikx-i\sigma t} = g\eta_{Eq}, \quad (1)$$

55 so that the fluid equilibrium height would be $|\eta_{Eq}| = H$, but with the half-space subsequently
 56 treated as completely rigid (unmoving).

57 2.1 Equations of an Elastic Sheet

58 Rheological properties of ice, whether on land or floating, are not simple—encompassing elastic,
 59 viscous, and plastic flow laws. MacAyeal and Sergienko (2013) propose that for time-scales of less
 60 than about 10 days, treating sea ice as elastic is appropriate and thus reasonable for describing
 61 ordinary semi-diurnal or diurnal tides. Discussion of long-period tides, or the evection-dominated
 62 ones in outer-solar system satellites, requires revisiting the question.

63 The ice is treated here as purely elastic with Lamé constants λ, μ and the physical and
 64 mathematical structure of the problem the free-mode analysis of Bromwich (1898), Press and
 65 Ewing (1951), and Ewing, Jardetzky and Press (1957, Ch. 5), but in the presence of a body-force.
 66 The Cartesian system governing an elastic plate is, {elastic1}

$$\bar{\rho} \frac{\partial^2 \bar{u}}{\partial t^2} = -\sigma^2 \bar{\rho} \bar{u} = (\lambda + \mu) \frac{\partial}{\partial x} \left(\frac{\partial \bar{u}}{\partial x} + \frac{\partial \bar{w}}{\partial z} \right) + \mu \nabla^2 \bar{u} + \bar{\rho} \frac{\partial U_T}{\partial x} \quad (2a) \quad \text{{elasta}}$$

$$\bar{\rho} \frac{\partial^2 \bar{w}}{\partial t^2} = -\sigma^2 \bar{\rho} \bar{w} = (\lambda + \mu) \frac{\partial}{\partial z} \left(\frac{\partial \bar{u}}{\partial x} + \frac{\partial \bar{w}}{\partial z} \right) + \mu \nabla^2 \bar{w} - g \bar{\rho} \quad (2b) \quad \text{{elastb}}$$

67 Variables \bar{u}, \bar{w} in the plate are *displacements*, not velocities. Barred variables, \bar{u} , etc., will refer
 68 to displacements in the ice layer, unbarred ones to corresponding *velocities* in the ocean. $\bar{\rho}$ is
 69 the density of ice, U has no vertical dependence in the thin ice layer and no y -dependence is
 70 considered. The background gravity g produces a resting static pressure $\bar{d} - \bar{\rho}gz$ in the ice.

71 What follows is in the spirit of the paper by Bromwich (1898) and who, as done in similar
 72 problems by Rayleigh and Love, defined the pressure as,

$$\bar{p}(x, z) = -\lambda \left(\frac{\partial \bar{u}}{\partial x} + \frac{\partial \bar{w}}{\partial z} \right), \quad (3)$$

73 taken as finite, but otherwise treated the medium as incompressible with,

$$\left(\frac{\partial \bar{u}}{\partial x} + \frac{\partial \bar{w}}{\partial z} \right) = 0, \quad (4) \quad \text{{nondiverge}}$$

74 and implying $\lambda \rightarrow \infty$. One advantage of this system is that it increases the resemblance be-
 75 tween the elastic and fluid equations. The sign of \bar{p} has been reversed here from the Bromwich
 76 definition, conventional in elasticity, in the interests of that analogy.

77 In any realistically ice-covered ocean, the ice sheet thickness would be a very small fraction
 78 of the tidal wavelength, suggesting the use of equilibrium thin-plate theory (e.g., Landau and

79 Lifschitz, 1987) instead of the dynamical wave equations. That course is not followed so as to
 80 make it possible to include the interesting situation in which much thicker ice sheets are disturbed
 81 by tides, a configuration perhaps existing in the outer solar system or amongst exoplanets.

82 2.2 Ocean Equations and Solutions

In a non-rotating, constant density, ρ , ocean, $-d \leq z \leq 0$, and using the familiar coordinate
 system with u, w being *velocities* in the positive x and z directions, {ocean1}

$$-i\sigma\rho u = -\frac{\partial(p - g\bar{\eta})}{\partial x} \quad (5a) \quad \{\text{xmomentum}\}$$

$$-i\sigma\rho w = -\frac{\partial p}{\partial z} - g\rho \quad (5b) \quad \{\text{hydrostatic}\}$$

$$\frac{\partial u}{\partial x} + \frac{\partial w}{\partial z} = 0 \quad (5c) \quad \{\text{continuity}\}$$

83 p' is the perturbation pressure. The system Eq. (5) is not assumed to be hydrostatic.

84 2.3 Non-dimensional System

85 Equations

With many dimensional quantities defining the system $(d, \bar{d}, \rho, \bar{\rho}, \mu, \sigma, k, g)$, it proves conve-
 nient to non-dimensionalize. A system equally useful in both the fluid and elastic media is not,
 however, obvious. The one chosen here is based upon the conventional time and space scales
 of ordinary water waves in a homogeneous fluid. Let all primed quantities be non-dimensional
 and,

$$T = 1/\sqrt{gk}, L = 1/k, U = L/T = \sqrt{\frac{g}{k}}, P = \rho g/k$$

$$\bar{U} = L, \bar{P} = \bar{\rho}g/k, d = d'/k, \bar{d} = \bar{d}'/k, \sigma = \sigma'\sqrt{gk}$$

$$(u, w) = U(u', w'), P = P'p', (\bar{u}, \bar{w}) = \bar{U}(\bar{u}', \bar{w}'), p' = \bar{P}\bar{p}'$$

and the elastic equations become, {iceeqsnondim}

$$\frac{\partial^2 \bar{u}'}{\partial t'^2} = -\frac{\rho}{\bar{\rho}} \frac{\partial \bar{p}'}{\partial x'} + \frac{1}{\gamma^2} \nabla'^2 \bar{u}' + H' \frac{\partial e^{ik'x'}}{\partial x'} \quad (6a)$$

$$\frac{\partial^2 \bar{w}'}{\partial t'^2} = -\frac{\rho}{\bar{\rho}} \frac{\partial \bar{p}'}{\partial z'} + \frac{1}{\gamma^2} \nabla'^2 \bar{w}' - 1 \quad (6b)$$

$$\frac{\partial \bar{u}'}{\partial x'} + \frac{\partial \bar{w}'}{\partial z'} = 0 \quad (6c)$$

86 with $\gamma^2 = \bar{\rho}g/\mu k = \left(\sqrt{g/k}/c_s\right)^2$, $c_s = \sqrt{\mu/\rho}$, $H' = Hk$, $k' = 1$. c_s is the shear wave-speed in
 87 the ice.

88 The corresponding non-dimensional fluid equations are then,

{nondimeqswate

$$\frac{\partial u'}{\partial t'} = -\frac{\partial p'}{\partial x'} + H' \frac{\partial e^{ik'x'}}{\partial x'} \quad (7a)$$

$$\frac{\partial w'}{\partial t'} = -\frac{\partial p'}{\partial z'} - 1 \quad (7b)$$

$$\frac{\partial u'}{\partial x} + \frac{\partial w'}{\partial z'} = 0 \quad (7c)$$

89 Although $k' = 1$, it is generally displayed below as a useful marker.

90 *Boundary Conditions*

91 Several (dimensional) boundary conditions must be considered. At the rigid sea floor, $z =$
92 $-d$,

$$w(-d) = 0.$$

93 At the ice-water interface, $z = \eta$, continuity of vertical displacement requires,

$$\bar{w}(0) = w(0) / (-i\sigma) = \eta$$

94 and which has been linearized about $z = 0$ as done in conventional wave theories. The conven-
95 tional water-wave dynamic boundary condition becomes one of continuity of normal stress,

$$-\bar{p}(0) + 2\mu \frac{\partial \bar{w}(0)}{\partial z} + g\bar{\rho}\bar{w}(0) = -p(0)$$

96 At the top of the ice-layer, at $z = \bar{d}$, the tangential stress must vanish,

$$\frac{\partial \bar{u}(\bar{d})}{\partial z} + \frac{\partial \bar{w}(\bar{d})}{\partial x} = 0$$

97 again linearized about $z = \bar{d}$. Also, the normal stress must vanish,

$$-\bar{p}(\bar{d}) + 2\mu \frac{\partial \bar{w}(\bar{d})}{\partial z} + g\bar{\rho}\bar{w}(\bar{d}) = 0.$$

Non-dimensionalizing as in the equations of motion,

{bcs_ice_ocean

$$0 = w'(-d'), \quad (8a) \quad \text{{nondimbcs}}$$

$$\bar{w}'(0) = \eta' / (-i\sigma'), \quad (8b)$$

$$-\bar{p}'(0) + \frac{2}{\gamma^2} \frac{\partial \bar{w}'(0)}{\partial z'} + \bar{w}'(0) = -p', \quad (8c)$$

$$\frac{\partial \bar{u}'(\bar{d}')}{\partial z'} + \frac{\partial \bar{w}'(\bar{d}')}{\partial x'} = 0, \quad (8d)$$

$$-\bar{p}'(\bar{d}') + \frac{2}{\gamma^2} \frac{\partial \bar{w}'(\bar{d}')}{\partial z'} + \bar{w}'(\bar{d}') = 0 \quad (8e)$$

98 From here on, the primes will be dropped, and unless otherwise specifically stated, all vari-
99 ables are non-dimensional (but figures are mainly presented in dimensional form).

3 Ocean Alone

For reference purposes, it proves helpful to first solve the tide problem in an ocean without an overlying ice sheet, and in an ice sheet without an underlying ocean, stuck fast to the half-space. Starting with the ocean alone, the problem is one in standard, forced, wave theory (Lamb, 1932; Kundu and Cohen, 2008), but is written out here to emphasize the parallel development in the ice.

Assuming conventional irrotational motion (tidal forcing has no curl), write $(u, w) = \nabla\varphi$, then

$$\varphi = \frac{\rho}{i\sigma} (p' - g\eta_{eq}) - \frac{g\rho z}{i\sigma}$$

and thus,

$$\nabla^2 p = g\nabla^2 \eta_{eq} = -g\rho k^2 H e^{ikx}$$

with solution,

$$p = -g\rho z + \rho g H e^{ikx} + \rho (E e^{kz} + F e^{-kz}) e^{ikx} \quad (9) \quad \{\text{pocean1}\}$$

with,

$$\varphi = \frac{\rho}{i\sigma} (E e^{kz} + F e^{-kz}) e^{ikx}. \quad (10) \quad \{\text{phioccean1}\}$$

The boundary condition $w(z = -d) = \partial\varphi(-d)/\partial z = 0$ requires, $F = E e^{-2kd}$ and then,

$$p(x, z) = -g\rho z + \rho g H e^{ikx} + \rho E (\cosh k(z + d)) e^{ikx} \quad (11) \quad \{\text{p1}\}$$

$$\varphi(x, z) = \frac{\rho E}{i\sigma} \cosh(k(z + d)) e^{ikx} \quad (12) \quad \{\text{phi1}\}$$

absorbing a constant factor into E .

Without overlying ice, the linearized free surface boundary conditions are,

$$-i\sigma\eta(x) = w(0) = \frac{kE}{i\sigma} (\sinh kd),$$

and Eq. (8ac) becomes $p = 0$ or,

$$-\eta + H + i\sigma \cosh kd = 0, \quad (13) \quad \{\text{surfbc1}\}$$

which is,

$$[-\sigma \cosh kd + k \sinh kd]E = -i\sigma H \quad (14) \quad \{\text{surfbc2}\}$$

If $H = 0$, the free solution produces the usual dispersion relationship for free surface waves, here

$$\sigma^2 = k \sinh kd, \quad k = 1,$$

116 and which would lead to resonance in Eq. (14).

117 Setting dimensional $k = 2\pi/6.3 \times 10^6$ (wavelength equal to the radius of the earth), and
 118 dimensional frequency as $\sigma = 2\pi/12.42\text{h}$ (the modern M₂ tide), Fig. 2 shows the ordinary
 119 tidal response, as a function of dimensional depth d , direct at low frequencies, inverted at high
 120 frequencies (small d) and a transition across resonance. The limit $kd \rightarrow 0$, shallow water, is
 121 readily used if desired.

122 4 Ice Alone

123 Consider an elastic ice sheet subject to tidal forcing overlying a rigid half-space. Two reasons
 124 motivate this approach: (1) To understand the direct response of the ice to tidal forcing and (2)
 125 To understand the sensitivity of that response to boundary conditions at the ice bed—exploring
 126 the hypothesis that measurements of tidal response in the Antarctic ice sheet might shed some
 127 light on the conditions at the generally inaccessible base of the ice sheet.

128 Absent any y -dependence—as is being assumed here—the displacements in the ice can be
 129 written generally as,

$$\bar{u} = \frac{\partial \bar{\varphi}}{\partial x} + \frac{\partial \bar{\psi}}{\partial z}, \quad \bar{w} = \frac{\partial \bar{\varphi}}{\partial z} - \frac{\partial \bar{\psi}}{\partial x}$$

130 that is as the gradient of a potential and the curl of a stream function and whose solutions are
 131 coupled through the boundary conditions. By Eq. (6c),

$$\nabla^2 \varphi = 0. \tag{15} \text{\{laplace2\}}$$

132 (Eq. (15) is the seismological P -wave equation in the limit of the P -wave speed, $\alpha \rightarrow \infty$.)

133 Assume all variables are now proportional to $\exp(-i\sigma t)$. Substituting $\bar{\psi}$ in the two momen-
 134 tum equations, dropping the forcing term, and cross-differentiating to eliminate the pressure
 135 produces,

$$\nabla^2 (\nabla^2 \bar{\psi} + \sigma^2 \gamma^2 \bar{\psi}) = 0,$$

136 or integrating

$$(\nabla^2 \bar{\psi} + \sigma^2 \gamma^2 \bar{\psi}) = M(x, z), \tag{16} \text{\{psi11\}}$$

137 where M is an harmonic function that will be set to zero. The solution then to Eq. (16) is

$$\bar{\psi}(x, z) = e^{ikx} (Ae^{imz} + Be^{-imz}), \quad m = \sqrt{\sigma^2 \gamma^2 - 1}$$

138 and the corresponding velocities are

$$\bar{u}^\psi(x, z) = ime^{ikx} (Ae^{imz} - Be^{-imz}), \quad \bar{w}^\psi(x, z) = -ie^{ikx} (Ae^{imz} + Be^{-imz}).$$

139 Substituting back into the homogeneous momentum equations produces $\bar{p}^\psi = 0$, p^ψ being the
 140 pressure associated with the stream function.

141 Let the solution to Eq. (15) be

$$\bar{\varphi}(x, z) = e^{ikx} (Ce^z + De^{-z})$$

Substituting φ into the non-dimensional momentum equations produces,

$$\begin{aligned} \frac{\partial^2}{\partial t^2} \frac{\partial \bar{\varphi}}{\partial x} &= -\frac{\rho}{\bar{\rho}} \frac{\partial \bar{p}}{\partial x} + He^{ikx}, \\ \frac{\partial^2}{\partial t^2} \frac{\partial \bar{\varphi}}{\partial z} &= -\frac{\rho}{\bar{\rho}} \frac{\partial \bar{p}}{\partial z} - 1 \end{aligned}$$

which leads to

$$\begin{aligned} \frac{\rho}{\bar{\rho}} \bar{p}(x, z) &= -\frac{\partial^2 \bar{\varphi}}{\partial t^2} + He^{ikx} - z & (17) \quad \{\text{pice}\} \\ &= \sigma^2 \bar{\varphi} + He^{ikx} - z \\ &= \sigma^2 (Ce^{kz} + De^{-kz}) e^{ikx} + He^{ikx} - z \end{aligned}$$

The boundary conditions at $z = 0$ are now $\bar{u}(0) = 0, \bar{w}(0) = 0$, together with those at $z = \bar{d}$
 are,

$$m(A - B) + k(C + D) = 0 \quad (18a) \quad \{\text{icea}\}$$

$$-ik(A + B) + k(C - D) = 0 \quad (18b) \quad \{\text{iceb}\}$$

$$(-m^2 + k^2) (Ae^{im\bar{d}} + Be^{-im\bar{d}}) + 2ik (Ce^{k\bar{d}} - De^{-k\bar{d}}) = 0 \quad (18c) \quad \{\text{icec}\}$$

$$\begin{aligned} A \left(\frac{2km}{\gamma^2} - 2ik \right) e^{im\bar{d}} + B \left(-\frac{2km}{\gamma^2} - 2ik \right) e^{-im\bar{d}} + C \left(-\sigma^2 + \frac{2k^2}{\gamma^2} + 2k \right) e^{k\bar{d}} + \\ D \left(-\sigma^2 + \frac{2k^2}{\gamma^2} + 2k \right) e^{-k\bar{d}} = H \quad (18d) \quad \{\text{iced}\} \end{aligned}$$

142 Taking $\mu = 2.3 \times 10^9$ (Squire et al., 1995), $\gamma \approx 2.1$. The dimensional values of $\bar{\eta} = \bar{w}(\bar{d})$ are
 143 shown in Fig. 3. For thin ice sheets, little or no tidal response occurs. As the ice thickens, the
 144 vertical displacement grows, as it does for high frequencies as the forcing phase speeds approach
 145 that for free shear waves in the ice. In the high frequency limit, a free solution which is a
 146 Rayleigh wave at the upper boundary of the ice sheet can produce a large response. Higher
 147 modes also are possible, although no real Earth tidal forcing exists with such phase speeds.

148 Much interest exists in the determination of the boundary conditions at the base of the
 149 ice sheet—a generally inaccessible place. The surface response of a continental ice sheet does
 150 depend upon those lower boundary conditions. For realistic Earth ice sheets, the forced response
 151 is sufficiently slight, whatever the basal boundary conditions, that the ability to measure the
 152 motions is somewhat doubtful, and thus the analysis is here placed in an Appendix.

5 Coupled Ice and Ocean

The non-dimensional system of boundary conditions can be written,

{iceandoceanal

$$-ikA - ikB + kC + kD + \frac{k}{i\sigma} \sinh(kd) E = 0, \quad (19a)$$

$$\left(\frac{2}{\gamma^2}km - 2ik\right) A + \left(-\frac{2}{\gamma^2}km - 2ik\right) B + \left(-\sigma^2 + \frac{2}{\gamma^2}k^2 + 2k\right) C + \left(-\sigma^2 + \frac{2}{\gamma^2}k^2 + 2k\right) D +$$

$$\left(i\sigma \cosh kd + \frac{k}{i\sigma} \sinh kd\right) E = \left(\frac{\bar{\rho}}{\rho} - 1\right) H, \quad (19b)$$

$$(-m^2 + k^2) A + (-m^2 + k^2) B + 2ik^2 C - 2ik^2 D = 0, \quad (19c)$$

$$(-m^2 + k^2) \left(Ae^{im\bar{d}} + Be^{-im\bar{d}}\right) + 2ik \left(Ce^{k\bar{d}} - De^{-k\bar{d}}\right) = 0, \quad (19d)$$

$$A \left(\frac{2km}{\gamma^2} - 2ik\right) e^{im\bar{d}} + B \left(-\frac{2km}{\gamma^2} - 2ik\right) e^{-im\bar{d}} + C \left(-\sigma^2 + \frac{2k^2}{\gamma^2} + 2k\right) e^{k\bar{d}} +$$

$$D \left(-\sigma^2 + \frac{2k^2}{\gamma^2} + 2k\right) e^{-k\bar{d}} = H \quad (19e)$$

with the last two equations unchanged from those for ice-alone. Setting $\bar{\rho}/\rho = 1$ is a useful approximation in 19b. Fig. 4 shows the contours, as a function of dimensionless σ and \bar{d} of η and $\bar{\eta}$ and Fig. 5 the corresponding lateral displacements.

6 Snowball Earth-Ocean

The question raised here is the nature and possible influence of tides in a snowball-Earth-like environment. In the modern ocean, tides are believed to provide a significant fraction of the energy required to sustain the observed three-dimensional circulation (Munk and Wunsch, 1998), roughly about 50%, with much of the energy used to provide the vertical mixing. Almost all of the rest comes from the wind-field—assumed absent in an ice-covered world—although this inference remains somewhat insecure owing to the complexity of the response to buoyancy forcing at top and bottom.

6.1 More Realism

Tides of a realistic ocean can be considerably more complex, involving rotation, interaction with boundaries, topography, and stratification. Some properties even of the non-rotating canal theory remain robust in the presence of all of these complications as the barotropic solutions (no stratification) remain governed by gravity-wave physics even where rotation is important. Resonances still appear, although they can be generated by the presence of sidewalls and not just from travelling-wave version seen here. Particle velocities are strongly influenced by rotation, as would

172 the boundary-layer between the ocean and the base of the ice sheet. In a non-rotating ocean,
173 an important mechanical boundary layer scale would be $(A/\sigma)^{1/2}$, becoming $\left(A/\sqrt{\sigma^2 - f^2}\right)^{1/2}$
174 where $f = 2\Omega \sin \phi$, Ω being the Earth’s rotation rate, and ϕ the latitude and A is a hypothetical
175 eddy-viscosity. At latitudes where $\sigma \approx f$ (the “inertial latitude”), the boundary layer physics
176 are distinct. For semi-diurnal tide constituents, that occurs only poleward of about 70° latitude,
177 but for diurnals it is at about 30° .

178 Numerous studies do exist of the boundary layer flows under ice in the Arctic (e.g., McPhee,
179 2002; Cole et al., 2014) where rotation tends to be important or dominant. For obvious reasons,
180 no observations exist of low-latitude sea ice-boundary layer interactions. Under-ice topography
181 can be very rough, and how to model the fluid interactions at low latitudes is not so clear.
182 A reasonable inference is that dissipation at the sea ice-water boundary would be at least as
183 important as that over abyssal planes today, and possibly considerably greater.

184 Of principle concern in discussing a snowball Earth is the topographic change: modern day
185 tides have a substantial fraction of their dissipation occurring in the shallow regions of the
186 continental margins (Egbert and Ray, 2001). Tidal response in shallow water, $d' \ll d$, is
187 largely a “co-oscillation” forced by the incoming tide from deeper water, rather than being a
188 direct response to the local forcing. In an ice-covered ocean with shallow margins, the deep
189 water tide would tend to undergo reflection as the ice-lid becomes ever-more effective as d'/\bar{d}
190 vanishes, and it is a reasonable surmise that continental margin dissipation would be greatly
191 reduced relative to today’s values (See Fig. 7.)

192 The second major tidal dissipation mechanism in the modern ocean is through baroclinic
193 conversion from the stratification and the presence of topography (e.g., Egbert and Ray, 2000). If
194 the snowball ocean is nearly unstratified as in the A2014 results, baroclinic conversion would also
195 be much reduced. Thus both major dissipation mechanisms become weaker, and the perhaps
196 paradoxical inference is that tides of an ocean with an ice-lid are likely to be considerably
197 stronger than they are today. An important caveat is that proximity to resonance can be a
198 sensitive function of the continental configuration and which will have changed greatly through
199 millions of years.

200 **6.2 Influence on the Circulation**

201 Consider the energetics of a snowball Earth ocean. The A2014 thermal forcing of $0.1\text{W}/\text{m}^2$
202 corresponds to a net power input of $3.6 \times 10^{13}\text{W}$, (36 Terrawatts, TW), an impressive amount of
203 energy compared to estimates of the energy required to maintain the modern ocean circulation
204 of roughly 2TW. On the other hand, the A2014 solutions depict a circulation with a thermal
205 range of about 0.4°C , and so the Carnot efficiency would be about $0.4/273 = 0.0015$, reducing the

206 useable power to about 50GW. This value is probably an upper bound on the efficiency (e.g.,
207 Peixoto and Oort, 1992). Is it possible that the tides of such an ocean would be energetically
208 competitive? Tidal forcing, in contrast, is a direct mechanical driver of kinetic energy; whether
209 a significant large-scale time-mean circulation is generated in practice has to be separated from
210 the question of overall energy input and dissipation.

211 In the modern ocean, particularly in shallow water, significant residual circulations result
212 from strong tidal flows (e.g. barotropic ones, Maier-Reimer, 1977; Zimmerman, 1978; and
213 baroclinic, King et al., 2009; Xing et al., 2011; Grisouard and Bühler, 2012). Continuing down
214 this speculative path, one might infer that shallower regions of a snowball ocean would produce
215 significant tidally-driven circulations. These would necessarily interact with any circulation
216 also present from convective driving. In general, the strength of rectified flows is inversely
217 proportional to the square of the water depth (e.g., Zimmermann, 1978) and would thus depend
218 upon just how much residual ocean water remained, as well as upon the bottom topography. Is
219 it possible that the circulation established by a barotropic or baroclinic tidal flow could compete
220 with that driven by the geothermal heating? Without actually answering that question, note
221 that a 1mm/s meridional barotropic flow, extending the width of the present Pacific Ocean
222 (10,000km) in a water depth of 2km, would produce a transport of about 20Sv, as compared to
223 the 30Sv maximum estimated by A2014 for the geothermal response.

224 Oceanic general circulation models usually have covert sources of energy, hidden in the
225 various sub-grid-scale eddy-mixing schemes. Explicit energetics would govern the breakdown of
226 an eddy-field derived from instabilities of the larger-scale flows. Other processes, such as those
227 generally ascribed to the breaking of internal waves, internal tides and related phenomena, would
228 however, have power sources hidden in eddy mixing coefficients. Most of this physics requires a
229 stratified fluid, and as the A2014 ocean is nearly unstratified, the role of tidal mixing is far from
230 obvious.

231 **7 Other Processes**

232 For obvious reasons, none of the results as applied to the snowball Earth are definitive, and
233 many unknowns and complications intervene. Some interesting physics problems arise. Among
234 other intriguing complications not discussed here are the role of the changed Earth rotation
235 rate and length of the month at times approaching -1GY when the day was probably about 22
236 hours long, and with about 13 synodic months in the year (Bills and Ray, 1999; Williams, 2000).
237 These changes are consequences of tidal friction and the resulting braking of the Earth's spin
238 over time.

239 If the modern ocean depth is reduced by half, and assuming that 600 million years ago that
 240 the salt amount in the ocean was similar to today, salinity would have roughly doubled to about
 241 7% of the water mass. A salty fluid, heated from below can be unstable to double-diffusive
 242 processes (see e.g., Turner, 1973; Brandt and Fernando, 1995) forming a layered circulation.
 243 Whether over millions of years that possibility persists, and what would be the consequences
 244 of any annual cycling at low latitudes in the ice-cover, has not been discussed. If some strati-
 245 fication does persist, then baroclinic conversion from the barotropic tide can occur, a spatially
 246 dependent mixing would arise, and a whole suite of theoretical problems can be defined includ-
 247 ing the baroclinic mean flows already alluded to above. Whether any possibility exists of an
 248 observational test of such interesting configurations is unclear, and we leave the problem as one
 249 of near-total speculation.

250 **Appendix. Basal Boundary Condition Sensitivity**

251 The equations governing an ice sheet frozen to a rigid underlying half-space are in Eqs. (??). If
 252 the the no-slip boundary condition (Eq. 18a) is replaced by one of no shear stress,

$$A(-m^2 + k'^2) + B(-m^2 + k'^2) + C(2ik'^2) + D(-2ik'^2) = 0.$$

253 Fig. 8 displays the dimensionalized solutions $\bar{u}(\bar{d})$ for an M_2 tidal forcing for the two boundary
 254 conditions. No-slip lateral motion is only about 1% of that for free-slip for realistic thicknesses
 255 which in principle would permit determination of the the appropriate boundary condition for
 256 surface displace (shear) measurements. On the other hand, the lateral displacement is of the
 257 order of microns, even for free slip, and the feasibility of detecting such small values in the
 258 presence of Earth noise is obscure.

259 *Acknowledgements*

References

- 261 Arbic, B. K., J. X. Mitrovica, et al. (2008). On the factors behind large Labrador Sea tides
262 during the last glacial cycle and the potential implications for Heinrich events. *Paleoceanography*
263 23(3): PA3211.
- 264 Ashkenazy, Y., H. Gildor, et al. (2014). Ocean circulation under globally glaciated snowball
265 Earth conditions: Steady-state solutions. *Journal of Physical Oceanography* 44(1): 24-43.
- 266 Bills, B. G. and R. D. Ray (1999). Lunar orbital evolution: A synthesis of recent results. *Geophysical*
267 *Research Letters* 26(19): 3045-3048.
- 268 Bromwich, T. I. A. (1898). On the Influence of Gravity on Elastic Waves, and, in particular
269 on the Vibrations of an Elastic Globe. *Proceedings of the London Mathematical Society* 1(1):
270 98-165.
- 271 Cole, S. T., M. L. Timmermans, et al. (2014). Ekman veering, internal waves, and turbulence
272 observed under Arctic Sea ice. *Journal of Physical Oceanography* 44(5): 1306-1328.
- 273 Davies, J. H. (2013). Global map of solid Earth surface heat flow. *Geochemistry Geophysics*
274 *Geosystems* 14: 4608-4622.
- 275 Egbert, G. D. and R. D. Ray (2000). Significant dissipation of tidal energy in the deep ocean
276 inferred from satellite altimeter data. *Nature* 405(6788): 775-778.
- 277 Egbert, G. D. and R. D. Ray (2001). Estimates of M-2 tidal energy dissipation from TOPEX/Poseidon
278 altimeter data. *Journal of Geophysical Research-Oceans* 106(C10): 22475-22502.
- 279 Ewing, W. M., W. S. Jardetzky, et al. (1957). *Elastic waves in layered media*. New York,,
280 McGraw-Hill.
- 281 Greenberg, R., P. Geissler, et al. (1998). Tectonic Processes on Europa: Tidal Stresses, Me-
282 chanical Response, and Visible Features. *Icarus* 135(1): 64-78.
- 283 Grisouard, N. and O. Buhler (2012). Forcing of oceanic mean flows by dissipating internal
284 tides. *Journal of Fluid Mechanics* 708: 250-278.
- 285 Harrison, W. D., K. A. Echelmeyer, et al. (1993). SHORT-PERIOD OBSERVATIONS OF
286 SPEED, STRAIN AND SEISMICITY ON ICE STREAM-B, ANTARCTICA. *Journal of Glaciol-*
287 *ogy* 39(133): 463-470.
- 288 Hoffman, P. F. and D. P. Schrag (2002). The snowball Earth hypothesis: testing the limits of
289 global change. *Terra Nova* 14(3): 129-155.
- 290 King, B., H. P. Zhang, et al. (2009). Tidal flow over three-dimensional topography in a stratified
291 fluid. *Physics of Fluids* 21(11).
- 292 Lamb, H. (1932). *Hydrodynamics*, Sixth ed, Dover, New York.
- 293 Lambeck, K. (1988). *Geophysical geodesy : the slow deformations of the earth*. Oxford England

294 New York, Clarendon Press ;
295 Oxford University Press.
296 Landau, L. D. and E. M. Lifshitz (1987). Fluid mechanics. Oxford, England ; New York,
297 Pergamon Press.
298 MacAyeal, D. R. and O. V. Sergienko (2013). The flexural dynamics of melting ice shelves. *Annals*
299 *of Glaciology* 54(63): 1-10.
300 Maier-Reimer, E. (1977). Residual circulation in the North Sea due to the M2-tide and mean
301 annual wind stress. *Deutsche Hydrographische Zeitschrift*, Jahrgang 30, 69-80.
302 McPhee, M. G. (2002). Turbulent stress at the ice/ocean interface and bottom surface hydraulic
303 roughness during the SHEBA drift. *Journal of Geophysical Research-Oceans* 107(C10).
304 Munk, W. and C. Wunsch (1998). Abyssal recipes II: energetics of tidal and wind mixing.
305 Munk, W. H. and G. J. F. MacDonald (1960). *The Rotation of the Earth: A Geophysical*
306 *Discussion*, Cambridge University Press, Cambridge.
307 Peixoto, J. P. and A. H. Oort (1992). *Physics of Climate*, Amer. Inst. Phys., New York.
308 Pollack, H. N. and S. J. Hurler, Johnson, J.R. (1993). Heat flow from the Earth's interior:
309 analysis of the global data set. *Reviews of Geophysics* 31: 267-280.
310 Thomas, R. H. (2007). Tide-induced perturbations of glacier velocities. *Global and Planetary*
311 *Change* 59(1-4): 217-224.
312 Turcotte, D. L. and G. Schubert (2002). *Geodynamics*. Cambridge ; New York, Cambridge
313 University Press.
314 Turner, J. S. (1973). *Buoyancy Effects in Fluids*, Cambridge Un. Press.
315 Williams, G. E. (2000). Geological constraints on the Precambrian history of Earth's rotation
316 and the Moon's orbit. *Reviews of Geophysics* 38(1): 37-59.
317 Zimmerman, J. T. F. (1978). Topographic generation of residual circulation by oscillatory (tidal)
318 currents. *Geophys. Astrophys. Fl. Dyn.* 11: 35-47.

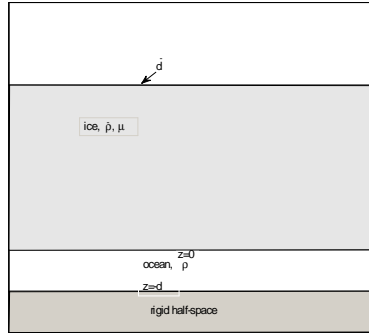


Figure 1: Defining schematic.

{sketch.eps}

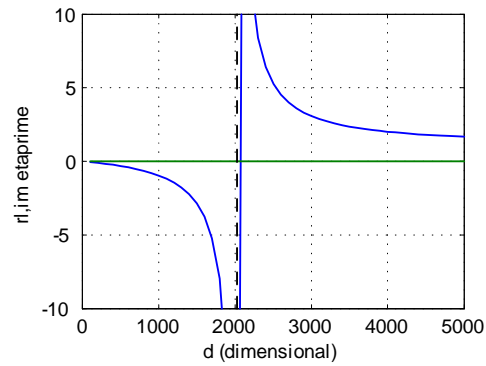


Figure 2: η (dimensional) for the ocean alone, with the resonance (vertical dashed line) at $\sigma/k = \sqrt{gd}$ apparent. Amplitude scale is truncated at the resonance.

{ocean_alone_e}

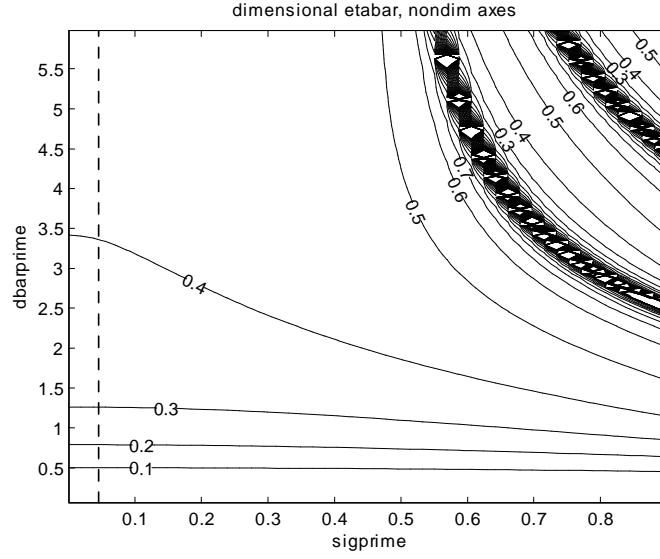


Figure 3: Contours of $\bar{w}(\bar{d})$ the vertical displacement at the top of the ice layer. Vertical dashed line is the M_2 tide frequency, far from the resonances visible in the upper-right corner.

{ice_along_dba

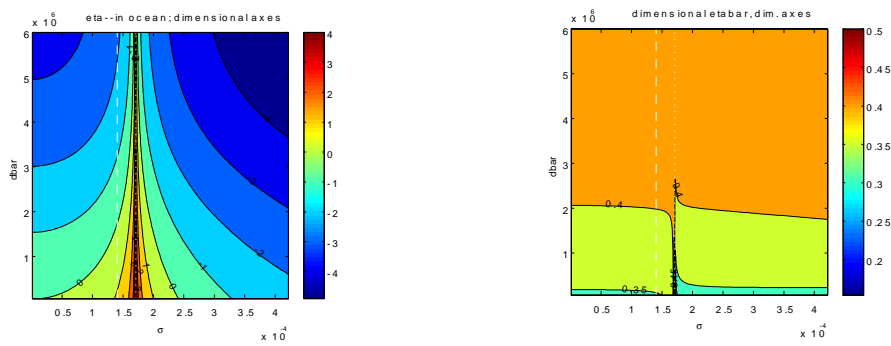


Figure 4: $\log_{10}(\eta)$, (left panel) in dimensional form and for $\bar{\eta}$ i with $d = 3000\text{m}$. White dashed line is the tidal frequency and dotted line is the resonance frequency.

{eta&etabar_mo

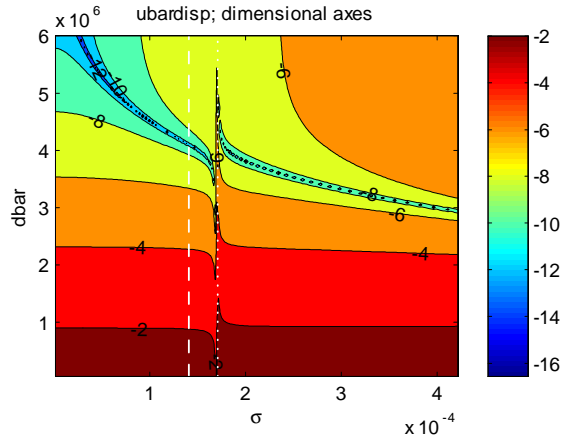


Figure 5: $\log_{19}(\bar{u}(z = \bar{d}))$ $d = 3000\text{m}$ with dimensional axes.

{ubardisp_ice&

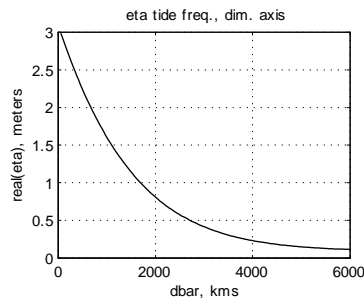


Figure 6: $\eta(\bar{d})$ at the tidal frequency, showing the decline in the ocean tide as the ice thickness grows. A value of 3m at $\bar{d} = 0$ is the result of near-resonant amplification of the ocean equilibrium value (1m). $d = 3000\text{m}$.

{eta_withice_d

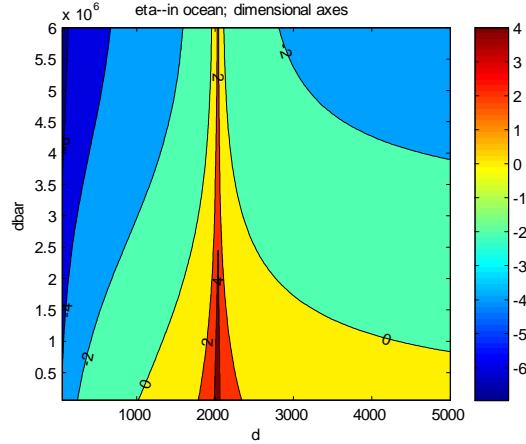


Figure 7: $\log_{10}(\eta)$ as a function of \bar{d}, d for the M_2 tidal frequency. For fixed d , the response diminishes with increasing ice thickness. The resonance, dominated by the ocean depth change is apparent. For fixed \bar{d} , η diminishes rapidly as the ocean depth is reduced and which would lead to reflection of incoming energy.

{eta_ice&ocean

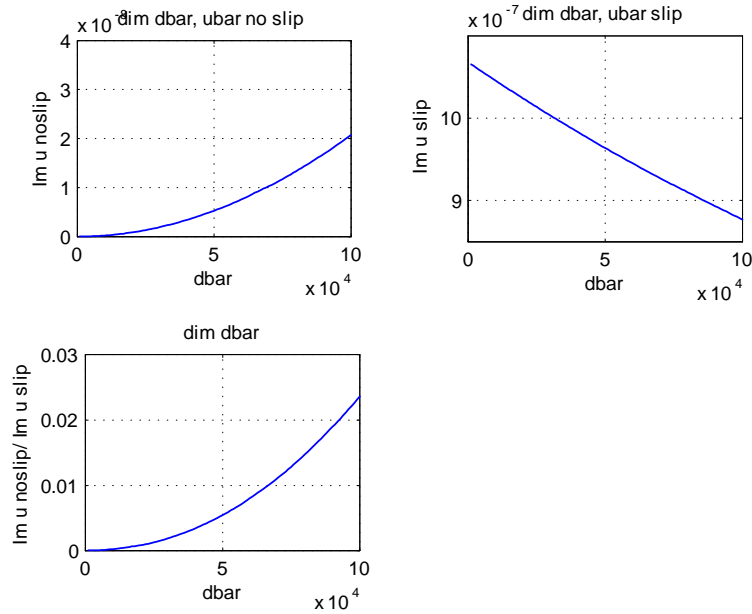


Figure 8: Dimensional $\bar{u}(\bar{d})$ versus \bar{d} for boundary conditions of no slip (upper left panel), free slip—no shear stress (upper right) and their ratio in an ice sheet in contact with a rigid half-space at $z = 0$.

{slip_noslip_u